Send Orders of Reprints at reprints@benthamscience.org

342 *Current Bioinformatics*, 2012, *7*, 342-351

Steered Molecular Dynamics-A Promising Tool for Drug Design

Mai Suan Li[1*] and Binh Khanh Mai[2]

[1]*Institute of Physics, Polish Academy of Sciences, Aleja Lotnikow 32/46, 02-668 Warszawa, Poland;*[2]*Institute for Computational Science and Technology, 6 Quarter, Linh Trung Ward, Thu Duc District, Ho Chi Minh City, Vietnam*

Abstract: About 15 years ago, the steered molecular dynamics (SMD) was used to probe binding of ligand to biomolecule surfaces but in terms of drug design this approach has only recently attached attention of researchers. The main idea of using SMD to screen out leads is based on the hypothesis that the larger is the force needed to unbind a ligand from a receptor the higher its binding affinity. Thus, instead of binding free energy, the rupture force defined as the maximum on the force-time/displacement profile, is used as a score function. In this mini-review, we discuss basic concepts behind the experimental technique atomic force microscopy as well as SMD. Experimental and theoretical works on the application of SMD to the drug design problem are covered. Accumulated evidences show that SMD is as accurate as the molecular mechanics-Poisson-Boltzmann surface area method in predicting ligand binding affinity but the former is computationally much more efficient. The high correlation level between theoretically determined rupture forces and experimental data on binding energies implies that SMD is a promising tool for drug design. Our special attention is drawn to recent studies on inhibitors of influenza viruses.

Keywords: Binding free energy, drug design, influenza virus, neuraminidase, rupture force, steered molecular dynamics.

I. INTRODUCTION

The design of one new drug approved by FDA takes about 15 years at expenses of nearly one billion USD. In order to shorten this process and make it less expensive, computer simulations can be used to identify leads and validate them as potential drugs. Top-leads predicted by computers may be recommended for further clinical trials on toxicity and drug-ability. From the physical point of view, the ligand binding affinity is defined by the binding energy of ligand to receptor. The binding energy can be estimated either by the docking method [1-20] or molecular dynamics (MD) simulations. The former method is very fast and can be used for screening potential leads from a large number of ligands available in various data bases [21]. However, its predictive power is low due to ignorance of receptor dynamics and a limited number of position trials of ligand.

There are several methods based on MD simulations like linear interaction energy (LIE) [22, 23], molecular mechanics/Poisson-Boltzmann (Generalized Born) surface area (MM/PB(GB)SA) [24, 25], free energy perturbation (FEP) [26] or thermodynamic integration (TI) [27] etc. All these methods are more accurate than the structure-based screening as they take into account dynamics of both ligand and receptor but they are not free from drawbacks associated with approximations they adopt. One of their disadvantages is that they are computationally much more expensive than the docking method and can only be used to study a very limited number of targets. Thus it is worth to work out a method which would be accurate enough but computationally less expensive compared to standard MD simulation methods.

*Address correspondence to this author at the Institute of Physics, Polish Academy of Sciences, Aleja Lotnikow 32/46, 02-668 Warszawa, Poland; Tel: +48-22-8436601; Fax: +48-22-8475223;
E-mail: masli@ifpan.edu.pl

Recently, motivated by the atomic force microscopy (AFM) experiments the steered molecular dynamics (SMD) [28, 29] has developed and applied to study mechanical unfolding of biomolecules [30, 31], transportation of ions [32, 33] and organic compounds through membrane channels [34, 35]. This method is also employed to probe unbinding pathways of ligand from its receptor [36, 37]. In this mini-review, we try to demonstrate that SMD is one of possible candidates to achieve two goals of drug design: more accurate than docking and more efficient than MD methods.

Basic concepts of the SMD will be described. Its application to to study ligand binding affinity of various complexes will be covered with focus on recent results obtained for the influenza virus problem. SMD is shown to be as powerful as MM-PBSA method in predicting binding affinity but about one order of magnitude faster.

II. STEERED MOLECULAR DYNAMICS METHOD

Inter- and intra-molecular forces are key to the stability of biomolecules. Up to now understanding of these forces is possible through indirect physical and thermodynamical measurements like crystallography, light scattering, nuclear magnetic resonance spectroscopy etc. In the case of ligand binding to receptor the binding energy E_{bind} is estimated via equilibrium association constant K_a constants using the equation $E_{bind} = -RT\ ln(K_a)$. Single molecule force spectroscopy experiments such as AFM [38], laser optical tweezers [39] and magnetic tweezers [40] can directly probe molecular forces and provide unexpected insights into the strength of forces driving various interactions responsible for the mechanical stability of bio-systems.

In standard single molecule force spectroscopy experiments one terminal (end) of a biomolecule is anchored to a surface, while another terminal is attached to a force sensor. A biomolecule is stretched by increasing the distance

2212-392X/12 $58.00+.00

between the surface and the force sensor. In the AFM case, the force sensor is a micron-sized cantilever. After the pioneering AFM experiment of Gaub *et al.* [41], a lot of experimental as well as theoretical works have been done on proteins, DNA and RNA [42, 43]. Biomolecules are pulled either with a constant force or by a force ramped with a constant loading rate. The force-extension curve of proteins under constant rate pulling has a saw-tooth shape due to domain by domain unfolding [44]. Schulten's group [45] was first to reproduce this remarkable result by SMD simulations.

To probe the binding affinity of ligand to receptor, one applies the external force to pull ligand from the binding pocket without fixing any atom of ligand (Fig. (**1a**)). As in the single molecule force spectroscopy the force experienced by ligand is proportional to the displacement of the cantilever. Under the force loaded with a constant rate the total energy of the receptor-ligand complex is as follows

$$E = E_{\text{receptor}} + E_{\text{ligand}} + E_{\text{receptor-ligand}} + E_{\text{force}}, \quad (1)$$

$$E_{force} = \frac{k}{2}(x - vt)^2.$$

Here E_{receptor},E_{ligand} and $E_{\text{receptor-ligand}}$ are energies of receptor, ligand and receptor-ligand interaction, respectively. Their forms depend on force fields used to describe the binding process. In AFM experiments, the spring constant of cantilever tip k is about 10 - 1000 pN/nm and x is the displacement of atom, which the force is applied to, from its initial position. v is the pulling speed while kv is the force loading rate. The ligand experiences the force $F = kx$ which is measured in experiments.

The breaking of hydrogen bonds (HB) requires a force $f \sim \varepsilon_H/a$. Assuming the hydrogen bond energy $\varepsilon_H \approx$ 1kcal/mol and typical distance between two atoms $a \approx$ 0.4 nm one needs force $f \sim$ 10 pN or a pulling rate $v \sim$ 100 nm/s to break a HB within one tenth of second using cantilever with k = 10 pN/nm. Suppose the binding pocket size ~ 1 nm and the experimental pulling rate $v \sim$ 100 nm/s, then one needs time $\sim 10^{-2}$ s to expose a ligand to the environment. Since within present computational facilities one can run all-atom MD simulations up to 1 μs, one has to pull ligand at least 10^4 times faster than in experiments. MD with high pulling speed or large constant force is called SMD. Nowadays, this method is implemented in most of softwares like GROMACS [46], AMBER [47], CHARMM [48] and NAMD [49].

Fig. (**1b**) shows a typical force-displacement profile for pulling ligand from the binding pocket with constant loading rate. Initially, the force experienced by ligand grows almost linearly in accord with the Hooke law. The peak is associated to sharp drop of not only the number of HBs but also the electrostatic and van der Waals (vdW) interactions [50]. The rupture force Fmax which defines the mechanical stability of ligand is directly related to unbinding but not binding process. However, intuitively one can hypothesize that the larger is the force needed to unbind a ligand from a receptor the higher its binding affinity. For comparison with experiments, one can use the following approximation

$$\Delta G_{\text{bind}} \approx -F_{\max} x_{\text{eff}} \quad (2)$$

Here x_{eff} is an effective displacement which presumably depends on systems and force fields used to treat them. Thus, in the SMD approach, instead of the binding free energy the rupture force is used as a score function to measure binding affinity. $F_{\max}$ cannot be directly compared with the ligand inhibitory capacity but it can be used to obtain relative binding affnities. Considering $W = -F_{\max}x_{\text{eff}}$ as the work performed in transition from bound to unbound state, one can show that Eq. (2) can be obtained in the first approximation in the cumulant expansion of the Jarzynski equality [51, 52].

Using the Bell-Evans-Ritchie argument [53, 54] one can show that Fmax depends on the pulling speed logarithmically, $F_{\max} \sim \ln(v)$ [55, 56]. Therefore, to compare binding properties of different complexes SMD simulations should be carried out at the same v. For loading rates of 10^0 - 10^5 pN/s, the rupture force varies between 10^0 - 10^2 pN [55].

As follows from studies of mechanical unfolding of proteins, the rupture force is sensitive to pulling direction [42, 57, 58]. Therefore, it is important to establish what pulling path should be chosen. If biomolecule is stretched with one point fixed, the force is directed along the vector connecting the anchored point and the point which the force is applied to. The situation becomes more complicated when a ligand is pulled from the binding site not keeping any atom fixed. In this case, one can not pull along arbitrary direction and an optimal pathway can be chosen [50] using, e.g. Caver 2.0 [59], a plugin of Pymol. The optimal path goes through the widest tunnel which is directed outside the binding pocket. The corresponding rupture force would be smallest among all possible pathways.

III. APPLICATION OF SMD TO LIGAND BINDING PROBLEM

A. Influenza Virus

Influenza, commonly referred to as the flu, is an infectious disease caused by RNA viruses of the family Orthomyxoviridae (the influenza viruses), that affects birds and mammals. Among three different classes A, B and C of influenza viruses, only type A has been observed to cause severe disease and pandemic [60]. In the last century, influenza pandemics occurred in 1918 (Spanish, H1N1), 1957 (Asian, H2N2) and 1968 (Hong Kong, H3N2) and killed millions of people [61, 62]. Recently, two types of influenza virus, H5N1 (avian flu) [63, 64] and H1N1 (swine flu) [65], have occurred and spread all over the world causing death in both people and millions of poultry. For the time being the swine flu H1N1 is in a post-pandemic phase, but no one can predict when the next pandemic will occur.

Influenza viruses A, B and C are very similar in overall structure (Fig. (**2**)). They are made of a viral envelope containing glycoproteins, wrapped around a central core. The central core contains the viral RNA genome and other proteins that package and protect this RNA. The influenza A genome contains 11 genes on eight pieces of RNA, encoding for 11 proteins: hemagglutinin (HA), neuraminidase (NA), M1, M2, NS1, NS2, NP, PA, PB1, PB1-F2 and PB2 [66].

A lipid envelop of the viral particle contains the two large glycoproteins HA and NA and the transmembrane

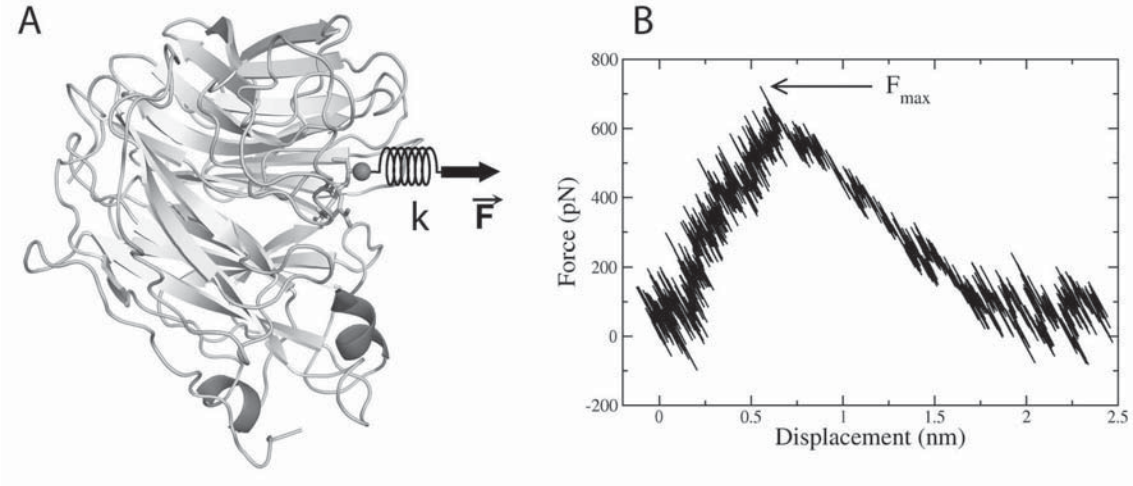

Fig. (1). (**A**) Schematic plot for pulling ligand from a receptor by applying the force $\vec{F}$ via the cantilever with the spring constant k. (**B**) Typical dependence of force experienced by ligand on the displacement from its initial position. The rupture force F_{max} serves as a score function for binding affinity.

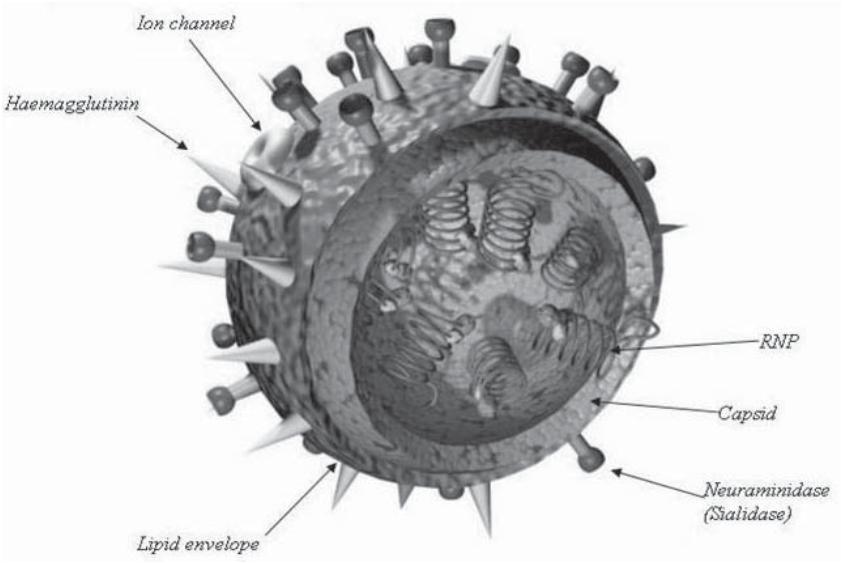

Fig. (2). Structure of the influenza virus. The hemagglutinin (HA) and neuraminidase (NA) proteins are shown on the surface of the particle. The ion channel associated with protein M2 is also shown. The viral RNAs that make up the genome are shown as red coils inside the particle and bound to Ribonuclear Proteins (RNPs). Reprinted from Wikipedia (http://en.wikipedia.org/wiki/Influenza).

protein M2. HA is a lectin that mediates binding of the virus to target cells and entry of the viral genome into the target cell, while NA plays a critical role in the release of progeny virus from infected cells by cleaving sugars that bind the mature viral particles [67, 68]. The integral membrane protein M2 is associated with the proton channel blocking of which can prevent the virus from being able to uncoat. Thus, HA, NA and M2 are targets for antiviral drugs [69-71]. Influenza A viruses are classified into subtypes based on antibody responses to HA and NA. There are 16 HA (H1-H16) and 9 NA (N1-N9) subtypes known [72], but only H1, H2 and H3, and N1 and N2 are commonly found in humans. A combination of these HA and NA subtypes is used to classify different strains such as H2N2, H5N1, H1N1 etc.

Currently, two types of drugs are licensed to treat influenza virus. The first class is a M2 inhibitor (amantadine and rimantadine) [73], which blocks the M2 proton channel of influenza virus [74]. These drugs are ineffective against influenza B [74, 75] and a number of amantadine-resistant cases have been reported [76]. The second class of drugs involves the NA inhibitors oseltamivir (Tamiflu) and zanamivir (Relenza), which are able to block the release of new virons from an infected cell [77]. These inhibitors are often effective against both influenza A and B virus [75], but some strains of avian H5N1 [78, 79] and swine pandemic H1N1 (pH1N1) influenza [80-82] are resistant to Tamiflu. Thus, it is vital to design a drug that is capable of treating both wild type (WT) influenza viruses as well as their mutants. In this mini-review, we focus on the application of

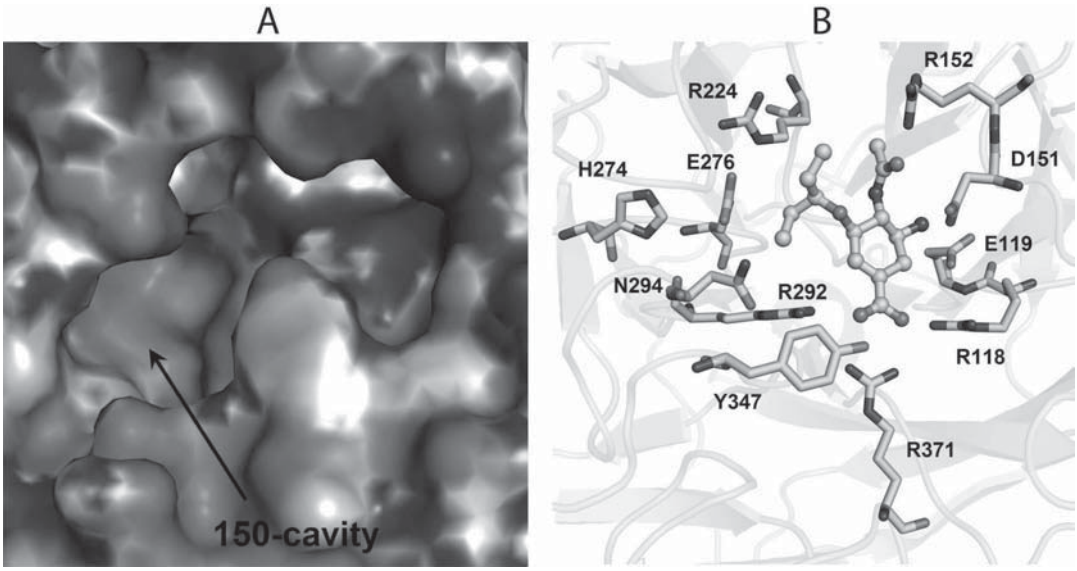

Fig. (3). Active site of H5N1 NA. The 150-cavity is absent in pH1N1.

SMD to study NA inhibitors of H5N1 and pH1N1. Recent results obtained for HA and M2 inhibitors may be found in the review of Rungrotmongkol *et al* [71].

Binding Site of NA of H5N1 and pH1N1

NA predominantly exists as a tetramer one chain of which is shown in Fig. (**1**). For H5N1 NA the 150-cavity, formed by open conformation of the 150-loop (residues 147-152), is adjacent to the sialic acid binding pocket (Fig. (**3**)) [83]. However, this cavity was not found in the pH1N1 NA [84]. The highly conserved binding pocket of H5N1 NA consists of 11 residues R118, E119 D151, R152, R224, H274, E276, R292, N294, Y347, and R371 (Fig. (**3**)). The active side of pH1N1 NA differs from H5N1 by only one residue at position 347 where Y347 is replaced by N347.

Nature of Ligand Binding to NA

Conventional MD simulations have been utilized to reveal key factors governing the binding affinity of inhibitors Oseltamivir, Zanamivir and Peramivir to WT and mutants (Y252H, N294S, and H274Y) of H5N1 and pH1N1 [71]. Their binding to H5N1, for instance, is mainly due to hydrogen bonding between the $-COO^-$ group with the three conserved arginines, R118, R292 and R371, as well as Y347.

Using the SMD method, one can show that the electrostatic interaction between ligand and receptor dominates over the van der Waals one [50, 85]. The hydrogen bonds alone do not define mechanical stability of ligand as they exist after passing the peak in the force-displacement profile [50, 86]. Thus, long range interactions also play the important role. Unbinding of tamiflu from the active site of WT H5N1 requires higher Fmax compared to pH1N1 case [50] or the Oseltamivir-pH1N1 NA complex is less stable than the H5N1 NA one. This is in accord with other theoretical works, where the binding free energies have been estimated using different force fields and methods [87-89]. The difference in binding affinities of Oseltavimir to pH1N1 and H5N1 lies in different residues at position 347. After the equilibration step of MD simulation, contrary to the H5N1 case, residue N347 in the active site of pH1N1 moves outward the binding site making its interaction with tamiflu weaker [50]. This assumption was confirmed by SMD simulations showing reduction of the number of HBs between the ligand and the receptor. A detailed geometrical picture on mechanical stability may be obtained monitoring time dependencies of distances between donors and acceptors of ligand and receptor [50]. Within the Gromos force field 43a1, the unbinding of Oseltamivir from pH1N1, for instance, is associated with breaking contacts between its and residues D151, E119, E227, and E277 of NA. It should be noted that the binding as well as unbinding process depend on force fields we use for simulations [90].

Recent Progress on Development of New NA Inhibitors

The tamiphosphor, the phosphonate congener of Oseltamivir and its analogs show more inhibitory potency than Osltamivir against the H1N1 and H5N1 [58]. This is because the replacement of the COO^- group by the $-PO_3^{2-}$ leads to more effective interactions with surrounding residues R118, Y347 and Y406 [91, 92]. Having used the open N1 conformation with the 150-cavity and 430-cavity adjacent to the sialic acid binding site [83] it has been suggested [93] that the modified Oseltavimir analogs with different numbers of hydroxyl group substitutions on the hydrophobic side chain and $-NHC(=NH_2^+)NH_2$ replacement on $-NH_3^+$ group showed increased binding affinity. Applying the virtual screening protocol to the NSC data set of about 250K ligands (see http://129.43.27.140/ncidb2/) McCammon's group [94] obtained 27 top hits for H5N1. The binding affinity of these top hits to pH1N1 has been examined by SMD method [50] which reveals that four ligands NSC-141562, NSC-5069, NSC-46080 and NSC-117079 (Fig. (**4**)) may be more potent than existing commercial drugs to cope the swine flu. Other potential leads have also been identified [95-98]. In the search for a more potent anti-H5N1 inhibitor, one should bear in mind

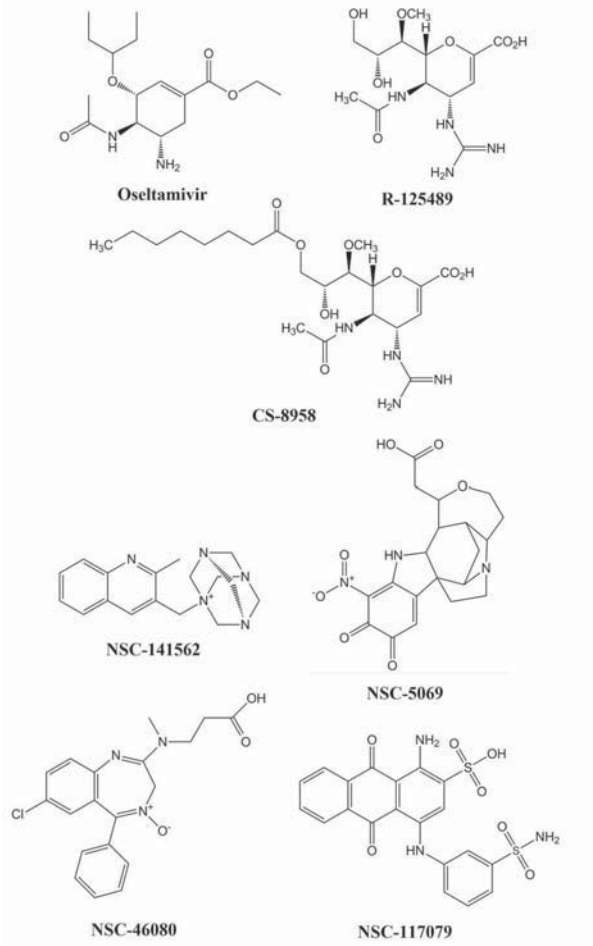

Fig. (4). Chemical structures of Oseltamivir and the new potent inhibitors against influenza NA target.

that ligands may in general bind to both "open" and "close" conformations of NA. But new leads presumably bind to the "open" conformation better than the "close" one as the latter is known from PDB for Tamiflu. In fact, it has been shown that the open form of crystal structure of NA is a reliable structural basis for designing derivatives of Oseltamivir as new potent drugs [98].

Experimentally Yamashita *et al* and other groups disclosed [99-103] that R-125489 and its prodrug CS-8958 (Fig. (**4**)) are promising drugs for treating both influenza A and B as well as their mutants. In an acidic environment, the long tail of CS-8958 is reduced as an ester group is replaced by a hydroxyl group or an acceptor group is transformed into the donor group. Using the density function theory, one can show that in this situation, the free energy of binding of R-125489 is lower than that of CS-8958 [86]. Consequently, CS-8958 easily adopts its active form in R-125489 with much higher binding affinity. In other words, the change in CS-8958 conformation reduces the steric effect and hydroxyl group can interact with polar residues in the active site leading to an increase in the binding affinity of R-125489 to all NAs. We note that intranasally administrated CS-8958 is quickly metabolized to R-125489 in the lungs and can be retained as a metabolite for a long time [99] (remember that intranasally administrated R-125489 is quickly removed from lung). This makes it possible for R-125489 to be used as a long-acting drug.

SMD is a Promising Tool for Drug Design

In studies on the unique beta-hydroxyacyl-ACP dehydratase of Plasmodium falciparum (PfFabZ) [104] and influenza virus [50], the good correlation between Fmax and experimental free energies was obtained only for 5-6 systems. In recent experiments [99-103], the binding affinity of R-125489 and CS-8958 (Fig. (**4**)) to 24 receptors (WT and mutants of H5N1, pH1N1, H3N8, H11N9, H8N4, H3N2, H11N6 and virus B) has been probed. In order to check the validity of SMD, the theoretical study of theses systems have been performed by Mai and Li [86]. In agreement with the experiments [99-103], R-125489 displays higher binding affinity than CS-8958 (Fig. (**5**)). The reason behind this difference lies in the repulsion between the long "tail" with 7 aliphatic carbons of CS-8958 and polar residues of receptor [86]. The excellent correlation between SMD and experiments (R = 0.97), obtained for the sufficiently large data set of 24 systems (Fig. **5**), strongly supports SMD as a very promising for drug design.

B. Other Systems

In the pioneer paper of Grubmuller, Heymann and Tavan [28], the force required to disassociate the streptavidin-biotin complex was calculated by SMD and the reasonable agreement with the AFM experiments [41] was obtained. The mechanical unbinding pathway of biotin (vitamin B_7, vitamin H) involves five major unbinding steps suggesting the importance of not only the HB network between receptor and ligand but also additional water bridges. Unbinding of retinoic acid from its receptor follows only one pathway and an alternative "forward door" pathway for binding [105]. The unbinding process of biovitin from avidin which is a tetrameric biotin-binding protein produced in the oviducts of birds, reptiles and amphibians deposited in the whites of their eggs, was also studied in detail [45]. The diversity of unbinding pathways has been observed. The SMD simulations were utilized for investigation of the unbinding of retinal from bacteriorhodophin [106] and the release of phosphate from the back door of actin [107, 108].

The entering and leaving processes of Huperzine A (HupA) binding with the long active-site gorge of Torpedo californica acetylcholinesterase (TcAChE) have been investigated [36]. SMD was also applied to study unbinding process of E2020 ((R,S)-1-benzyl-4-[(5,6-dimethoxy-1-indanon)-2-yl]-methylpiperidine) from the same receptor TcAChE [109]. Nanosecond scale simulations with different pulling velocities revealed that contrary to inhibitor HupA that undergoes the greatest barrier located at the bottleneck of the gorge, the major resistance preventing E2020 from leaving the gorge is from the peripheral anionic site, where E2020 interacts intensively with several aromatic residues through its benzene ring. This results in a strong direct hydrogen bond and a water bridge with Ser286 via its O24

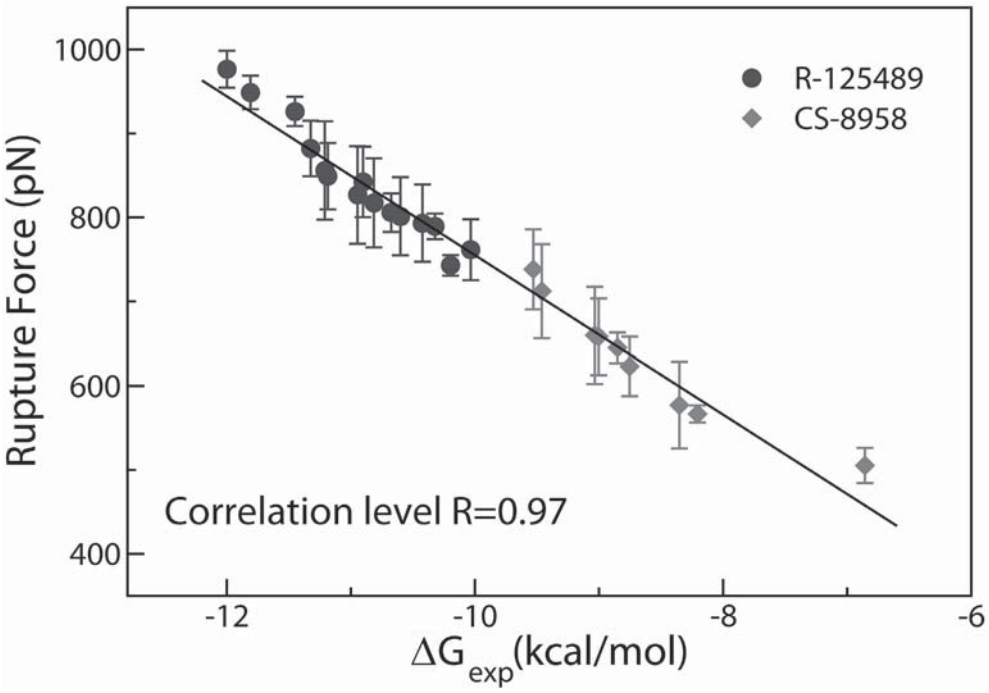

Fig. (5). Correlation between rupture forces and experimental binding energies of R-125489 and CS-8958 to NAs of influenza virus [99]. Results for Fmax are averaged over 4 pulling trajectories. The linear fit is $y = -191.103 - 94.611x$ with correlation level $R = 0.97$. Taken from Ref. [86].

causing the large rupture force ≈ 550 pN [109]. The binding affinity of non-nucleoside inhibitor α-APA to human immunodeficiency virus type one reverse transcriptase (HIV-1 RT) has been also probed [110].

SMD was used to explore the process of Ca^{2+} dissociation from the EF-hand motifs of the C-terminal lobe of calmodulin [111]. Based on an analysis of the pulling forces, the dissociation sequences and the structural changes, one can show that the Ca^{2+}-coordinating residues lose their binding to Ca^{2+} in a stepwise fashion.

The pulling simulations have been carried out to study the possible dissociation pathways of typical type II inhibitor imatinib from its targeting protein kinases c-Kit and Abl [112]. The most favorable pathway for imatinib dissociation corresponds to the ATP-channel rather than the relatively wider allosteric-pocket-channel, which is mainly due to the different van der Waals interaction that the ligand suffers during dissociation. The pathway for glutamine to release from glutamine-binding proteins was revealed by SMD simulations [113].

Plasmodium falciparum mamalia infections are estimated to be about half a billion annually continuing to threaten lives in tropical and subtropical zones of the world [114]. The unique beta-hydroxyacyl-ACP dehydratase of Plasmodium falciparum was shown to be a target for antimalarial drug design. Combining the docking with single-molecule pulling simulations Colizzi *et al.* [104] have studied the binding affinity of six monohydroxylated flavones to PfFabZ. In agreement with the experiments [104] SMD-derived force profiles have shown to discern active from inactive compounds.

The estrogen receptors (ERs) belong to a superfamily named nuclear receptors, which play crucial roles in the human body, including the growth and differentiation of the reproductive system, the central nervous system, and the skeletal system. ERs have two subtypes, ERα and ERβ. Ligands such as WAY-244 and Genistein exert their regulatory effects via binding ERs, which induces conformational changes in the protein structure and produces the physiological effects of the receptor. Unbinding pathways of these ligands have been probed by SMD [115] indicating that His524/475 in ERα/ERβ acted as a "gatekeeper" during the unbinding process.

SMD simulations of ligand-receptor interaction in lipocalins have been performed [116]. The difference in binding mechanism of retinol to its binding protein (RBP) and digoxigenin to an engineered lipocalin, DigA16, have been studied in detail using 10-20 ns simulations. Digoxigenin is bound deep inside the cavity of DigA16 and forms several stable hydrogen bonds in addition to the hydrophobic van der Waals interaction with the aromatic side-chains, while the strongly hydrophobic receptor site of RBP differs considerably from DigA16. Here, the main source of ligand attraction comes from the phenyl side-chains.

Dipeptidyl peptidase IV is an important target for the treatment of Type II diabetes mellitus as it is responsible for the secretion of insulin after dietary intake. Its crystal structure [117] suggests that there are two possible pathways to the active site, a side opening and a beta propeller opening. The pulling simulations have been carried to explore release of inhibitor Q448 from the active site [118].

The comparisons of results, obtained for force-profile, mechanical work and potentials of mean force suggest that the side opening is more favorable for the inhibitor to pass through.

IV. COMPARISON OF SMD WITH OTHER METHODS

The results obtained for ΔG_{bind} depend not only on force fields but also on methods [90, 119]. This is because different approaches adopt different approximations. In LIE method, for instance, the binding free energy is calculated using the interaction energy between ligand and its surroundings in bound and unbound state. However, in most cases, one needs to know a priori binding affinities from experiments and the success of this method crucially depends on empirical parameters. A more accurate estimation of binding energy can be obtained by the FEP/TI method but it is very CPU time consuming.

The comparison of SMD with the MM-PBSA method has been carried out studying the binding affinity of seven ligands (Tamiflu, Relenza, Peramivir, and four ligands 141562, 5069, 46080 and 117079 from the NSC) to pH1N1 NA [50]. Since, the correlation between ΔG_{bind} and F_{max} for these compounds is very high (R = 0.95), SMD is expected to be as good as MM/PBSA in drug design. Nevertheless, to cement this conclusion, one has to have better statistics than just seven systems. The advantage of SMD is that it is about 30-fold faster than MM-PBSA if we choose the pulling speed v = 0.005 mn/ps [50]. Thus, the number of ligands that may be studied by this method is about one order of magnitude larger than other MD methods. Even though, SMD method cannot be used to screen leads from large ligand data bases as the docking technique [21]. Another disadvantage of SMD is that it can predict relative binding affinities but not the absolute ones as in other MD approaches. One should bear in mind also some drawbacks of these methods. For instance, MM-PBSA is quite good in ranking binding affinity but its performance is relatively poor in some cases [120, 121]. This is due to the approximation in which the explicit solvent is represented as a continuum having a relatively high dielectric constant, while the protein and ligand are viewed as point charges projected onto a grid in a low dielectric constant.

V. CONCLUSION

The problem of calculating the potential of mean force (the free energy along a reaction coordinate) by combination of SMD with Jarzynski's equality [52, 122] and weighted histogram analysis [123, 124] has not been discussed. This is partially because in terms of binding affinity the potential of mean force does not provide much more insight compared to the rupture force. We have reviewed results obtained by the SMD where the ligand is pulled along one direction. Recently, a modified method with adjusting pulling direction to search an optimum trajectory of ligand dissociation has been proposed [125, 126]. The pathway obtained by this method has less dissociation time, smaller rupture force and lower energy barrier than that by the conventional SMD. The so called hybrid SMD-docking method [127] that uses the score different from ΔG_{bind} and F_{max} also looks promising.

The complete reconstruction of an enzyme-inhibitor binding process by standard molecular dynamics simulations is computationally very expensive. For instance, to get reasonable description of benzamidine binding to trypsin one has to perform 495 molecular dynamics simulations of free ligand binding of 100 ns each, 187 of which produced binding events [128]. Therefore, new ideas for further improvement of SMD would be highly desirable for drug design.

CONFLICT OF INTEREST

The authors confirm that this article content has no conflicts of interest.

ACKNOWLEDGEMENTS

We thank Truc Trang Nguyen, Man Hoang Viet and Son Tung Ngo for many useful discussions and E. P. O'Brien Jr for the critical reading of the manuscript. This work was supported by the Department of Science and Technology of the Ho Chi Minh City, Vietnam and Narodowe Centrum Nauki in Poland grant No 2011/01/B/NZ1/01622.

.

REFERENCES

[1] Lengauer T, Rarey M. Computational methods for biomolecular docking. Curr Opin Struct Biol 1996; 6: 402-406.
[2] Jorgensen WL. Efficient drug lead discovery and optimization. Account Chem Res 2009; 42: 724-733.
[3] Rosenfeld RJ, Goodsell DS, Musah RA, Morris GM, Goodin DB, Olson AJ. Automated docking of ligands to an artificial active site: augmenting crystallographic analysis with computer modeling. J Comput Aided Mol Des 2003; 17: 525-536.
[4] Goodsell DS, Morris GM, Olson AJ. Automated docking of flexible ligands: applications of AutoDock. J Mol Recognit. 1996; 9: 1-5.
[5] Ewing TJA, Makino S, Skillman AG, Kuntz ID. DOCK 4.0: search strategies for automated molecular docking of flexible molecule databases. J Comput Aided Mol Des 2001; 15: 411-428.
[6] Rarey M, Kramer B, Lengauer T, Klebe G. A fast flexible docking method using an incremental construction algorithm. J Mol Biol 1996; 261: 470-489.
[7] Kramer B, Rarey M, Lengauer T. Evaluation of the FLEXX incremental construction algorithm for protein-ligand docking. Proteins 1999; 37: 228-241.
[8] Yang JM. Development and evaluation of a generic evolutionary method for protein-ligand docking. J Comput Chem 2004; 25: 843-857.
[9] Yang JM, Chen CC. GEMDOCK: a generic evolutionary method for molecular docking. Proteins 2004; 55: 288-304.
[10] Friesner RA, Banks JL, Murphy RB, *et al.* Glide: a new approach for rapid, accurate docking and scoring. 1. Method and assessment of docking accuracy. J Med Chem 2004; 47: 1739-1749.
[11] Halgren TA, Murphy RB, Friesner RA, *et al.* Glide: a new approach for rapid, accurate docking and scoring. 2. Enrichment factors in database screening. J Med Chem 2004; 47: 1750-1759.
[12] Kirkpatrick P. Virtual screening: Gliding to success. Nat Rev Drug Discov 2004; 3: 299-9.
[13] Krovat EM, Steindl T, Langer T. Recent Advances in Docking and Scoring. Curt Computer- Aided Drug Design 2005; 1: 93-102.
[14] Friesner RA, Murphy RB, Repasky MP, *et al.* Extra precision glide: docking and scoring incorporating a model of hydrophobic enclosure for protein-ligand complexes. J Med Chem 2006; 49: 6177-6196.
[15] Verdonk ML, Cole JC, Hartshorn MJ, Murray CW, Taylor RD. Improved protein-ligand docking using GOLD. Proteins 2003; 52: 609-623.
[16] Joy S, Nair PS, Hariharan R, Pillai MR. Detailed comparison of the protein-ligand docking effciencies of GOLD, a commercial package and ArgusLab, a licensable freeware. In Silico Biol 2006; 6: 601-605.

[17] Thomsen R, Christensen MH. MolDock: A New Technique for High-Accuracy Molecular Docking. J Med Chem 2006; 49: 3315-3321.

[18] Jain AN. Surflex: fully automatic flexible molecular docking using a molecular similarity-based search engine. J Med Chem 2003; 46: 499-511.

[19] Mitrasinovic PM. On the structure-based design of novel inhibitors of H5N1 influenza A virus neuraminidase (NA). Biophys Chem 2009; 140: 35-38.

[20] Mihajlovic ML, Mitrasinovic PM. Applications of the ArgusLab4/AScore protocol in the structure-based binding affnity prediction of various inhibitors of group-1 and group-2 influenza virus neuraminidases (NAs). Mol Simulation 2009; 35: 311-324.

[21] Ravindranathan KP, Mandiyan V, Ekkati AR, Bae JH, Schlessinger J, Jorgensen WL. Discovery of novel fibroblast growth factor receptor 1 kinase inhibitors by structure-based virtual screening. J Med Chem 2010; 53: 1662-1672.

[22] Åqvist J, Medina1 C, Samuelsson JE. A new method for predicting binding affnity in computer-aided drug design. Protein Eng 1994; 7: 385-391.

[23] Hansson T, Marelius J, Åqvist J. Ligand binding affinity prediction by linear interaction energy methods. J Comput-Aided Mol Des 1998; 12: 27-35.

[24] Srinivasan J, III TEC, Cieplak P, Kollman PA, Case DA. Continuum solvent studies of the stability of DNA, RNA, and Phosphoramidate-DNA helices. J Am Chem Soc 1998; 120: 9401-9409.

[25] Kollman PA, Massova I, Reyes C, *et al.* Calculating structures and free energies of complex molecules: combining molecular mechanics and continuum models. Acc Chem Res 2000; 33: 889-897.

[26] Zwanzig RW. High-Temperature Equation of State by a Perturbation Method. I. Nonpolar Gases. J Chem Phys 1954; 22: 1420-1426.

[27] Kirkwood JG. Statistical Mechanics of Fluid Mixtures. J Chem Phys 1935; 3: 300-313.

[28] Grubmüller H, Heymann B, Tavan P. Ligand Binding: Molecular Mechanics Calculation of the Streptavidin-Biotin Rupture Force. Science 1996; 271: 997-999.

[29] Isralewitz B, Gao M, Schulten K. Steered molecular dynamics and mechanical functions of proteins. Curr Opin Struct Biol 2001; 11: 224-230.

[30] Isralewitz B, BaudryJ, Gullingsrud J, Kosztin D, Schulten K. Steered molecular dynamics investigations of protein function. J Mol Graphics Modell 2001; 19: 13-25.

[31] Lu H, Isralewitz B, Krammer A, Vogel V, Schulten K. Unfolding of titin immunoglobulin domains by steered molecular dynamics simulation. Biophys J 1998; 75: 662-671.

[32] Giorgino T, Fabritiis GD. A High-Throughput steered molecular dynamics study on the free energy profile of ion permeation through Gramicidin A. J Chem Theory Comput 2011; 7: 1943-1950.

[33] Gwan JF, Baumgaertner A. Cooperative transport in a potassium ion channel. J Chem Phys 2007; 127: 045103.

[34] Hénin J, Schulten ETK, Chipot C. Diffusion of Glycerol through Escherichia coli Aquaglyceroporin GlpF. Biophys J 2008; 94: 832-839.

[35] Jensen MØ, Park S, Tajkhorshid E, Schulten K. Energetics of glycerol conduction through aquaglyceroporin GlpF. Proc Natl Acad Sci 2002; 99: 6731-6736.

[36] Xu Y, Shen J, Luo X, Silman I, Sussman JL, Chen K, Jiang H. How does huperzine A enter and leave the binding gorge of acetylcholinesterase? Steered molecular dynamics simulations,. J Am Chem Soc 2003; 125: 11340-11349.

[37] Shen L, Shen J, Luo X, *et al.* Steered molecular dynamics simulation on the binding of NNRTI to HIV-1RT. Biophys J 2003; 84: 3547-3563.

[38] Binnig G, Quate CF, Berger CH. Atomic force microscope. Phys Rev Lett 1986; 56: 930-933.

[39] Simmons R, Finer J, Chu S, Spudich J. Quantitative measruments of force and displacement using an optical trap. Biophys J 1996; 70: 1813-1822.

[40] Amblard F, Yurke B, Pargellis A, Leibler S. Magntic manipulation for studying local rheology and micromechanical properties of biological systems. Rev Sci Instrum 1996; 67: 1-10.

[41] Florin EL, Moy VT, Gaub HE. Adhesion forces between individual ligand-receptor pairs. Science 1994; 264: 415-417.

[42] Kumar S, Li MS. Biomolecules under mechanical force. Phys Reports 2010; 486: 1-74.

[43] Li MS. Secondary structure, mechanical stability and location of transition state of proteins. Biophys J 2007; 93: 2644-2654.

[44] Rief M, Gautel M, Oesterhelt F, Fernandez JM, Gaub HE. Reversible unfolding of individual titin immunoglobulin domains by AFM. Science 1997; 276: 1109-1112.

[45] Izrailev S, Stepaniants S, Balsera M, Oono Y, Schulten K. Molecular dynamics study of unfolding of avidin-biotin complex. Biophys J 1997; 72: 1568-1581.

[46] Hess B, Kutzner C, van der Spoel D, Lindahl E. GROMACS 4: Algorithms for highly effcient, load-balanced, and scalable molecular simulation. J Chem Theor Comp 2008; 4: 435-447.

[47] Ponder JW, Case DA. Force fields for protein simulations. Adv Prot Chem 2003; 66: 27-85.

[48] MacKerell JAD, Bashford D, Bellott M, *et al.* All-atom empirical potential for molecular modeling and dynamics Studies of proteins. J Phys Chem B 1998; 102: 3586-3616.

[49] Phillips JC, Braun R, Wang W, *et al.* Scalable molecular dynamics with NAMD. J Comput Chem 2005; 26: 1781-1802.

[50] Mai BK, Viet MH, Li MS. Top-Leads for Swine Influenza A/H1N1 Virus Revealed by Steered Molecular Dynamics Approach. J Chem Inf Model 2010; 50: 2236-2247.

[51] Jarzynski C. Nonequilibrium equality for free energy differences. Phys Rev Lett 1997; 78: 2690-2693.

[52] Park S, Khalili-Araghi F, Tajkhorshid E, Schulten K. Free energy calculation from steered molecular dynamics simulations using Jarzynski's equality. J Chem Phys 2003; 119: 3559- 3566.

[53] Bell GI. Models for the specific adhesion of cells to cells. Science 1978; 100: 618-627.

[54] Evans E, Ritchie K. Dynamics strength of molecular adhesion bonds. Biophys J 1997; 72: 1541-1555.

[55] Merkel R, Nassoy P, Leung A, Ritchie K, Evans E. Energy landscapes of receptor-ligand bonds explored with dynamic force spectroscopy. Nature 1999; 397: 50-53.

[56] Heymann B, Grubmuller H. AN02/DNP-hapten unbinding forces studied by molecular dynamics atomic force microscopy simulations. Chem Phys Lett 1999; 303: 1-9.

[57] Kouza M, Hu CK, Li MS. New force replica exchange method and protein folding pathways probed by force-clamp technique. J Chem Phys 2008; 128: 045103.

[58] Carrion-Vazquez M, Li HB, Lu H, Marszalek PE, Oberhauser AF, Fernandez JM. The mechanical stability of ubiquitin is linkage dependent. Nat Struct Biol 2003; 10: 738-743.

[59] Petrek M, Otyepka M, Banas P, Kosinova P, Koca1 J, Damborsky J. CAVER: a new tool to explore routes from protein clefts, pockets and cavities. BMC Bioinformatics 2006; 7: 316.

[60] Kilbourne ED. Influenza pandemics of the 20th century. Emer Infect Dis 2006; 12: 9-14.

[61] Palese P. Influenza: old and new threats. Nat Med 2004; 10: S82-S87.

[62] Hsieh YC, Wu TZ, Liu DP, *et al.* Influenza pandemics: past, present and future. J Formos Med Assoc 2006; 105: 1-6.

[63] Ferguson NM, Fraser C, Donnelly CA, Ghani AC, Anderson RM. Public health risk from the avian H5N1 influenza epidemic. Science 2004; 304: 968-969.

[64] Yen HL, Webster RG. Pandemic influenza as a current threat. Curr Top Microbiol Immunol 2009; 333: 3-24.

[65] Neumann G, Noda T, Kawaoka Y. Emergence and pandemic potential of swine-origin H1N1 influenza virus. Nature 2009; 459: 931-939.

[66] Ghedin E, Sengamalay NA, Shumway M, *et al.* Large-scale sequencing of human influenza reveals the dynamic nature of viral genome evolution. Nature 2005; 437: 1162-1166.

[67] Suzuki Y. Sialobiology of influenza molecular mechanism of host range variation of influenza viruses. Biol Pharm Bull 2005; 28: 399-408.

[68] Murphy BR, Webster RG. in Fields Virology. 3rd ed. Philadelphia: Lippincott-Raven; 1996.

[69] Wilson JC, von Itzstein M. Recent strategies in the search for new anti-influenza therapies. Curr Pharm Targets 2003; 4: 389-408.

[70] Kobasa D, Kodihalli S, Luo M, *et al.* Amino acid residues contributing to the substrate specificity of the influenza A virus neuraminidase. J Virol 1999; 73: 6743-6751.

[71] Rungrotmongkol T, Yotmanee P, Nunthaboot N, Hannongbua S. Computational studies of influenza A virus at three important targets: Hemagglutinin, Neuraminidase and M2 protein. Curr Pharm Design 2011; 17: 1720-1739.

[72] WHO. A revision of the system of nomenclature for influenza viruses: a WHO memorandum. Bull World Health Organ 1980; 58: 585-591.

[73] Hay AJ, Wolstenholme AJ, Skehel JJ, Smith MH. The molecular basis of the specific anti-influenza action of amantadine. EMBO J 1985; 4: 3021-3024.

[74] Pinto LH, Lamb RA. The M2 proton channels of influenza A and B viruses. J Biol Chem 2006; 281: 8997-9000.

[75] Stephenson I, Nicholson KG. Chemotherapeutic control of influenza. J Antimicrob Chemother 1999; 44: 6-10.

[76] Monto AS, Arden NH. Implications of viral resistance to amantadine in control of influenza A. Clin Infect Dis 1992; 15: 362-367.

[77] Moscona A. Neuraminidase inhibitors for influenza. N Engl J Med 2005; 353: 1363-1373.

[78] Le QM, Kiso M, Someya K, *et al.* Avian flu: isolation of drug-resistant H5N1 virus. Nature 2005; 437: 1108.

[79] Webster RG, Govorkova EA. H5N1 influenza-continuing evolution and spread. N Engl J Med 2006; 355: 2174-2177.

[80] Centers for Disease Control and Prevention (CDC). Oseltamivir-resistant novel influenza A (H1N1) virus infection in two immunosuppressed patients - Seattle, Washington, 2009. MMWR Morb Mortal Wkly Rep. 2009; 58: 893-896.

[81] Centers for Disease Control and Prevention (CDC). Oseltamivir-resistant 2009 pandemic influenza A (H1N1) virus infection in two summer campers receiving prophylaxis - North Carolina, 2009. MMWR Morb Mortal Wkly Rep. 2009; 58: 969-972.

[82] WHO. Pandemic (H1N1) 2009 briefing note 1;. *http://www.who.int/csr/disease/ swineflu/notes/h1n1 antiviral resistance 20090708/en/index.html*. (accessed July 8, 2009).

[83] Russell RJ, Haire LF, Stevens DJ, *et al.* The structure of H5N1 avian influenza neuraminidase suggests new opportunities for drug design. Nature 2006; 443: 45-49.

[84] Li Q, Qi JX, Zhang W, *et al.* The 2009 pandemic H1N1 neuraminidase N1 lacks the 150-cavity in its active site. Nat Struct Mol Biol 2010; 17: 1266-1268.

[85] Le L, Lee EH, Hardy DJ, Truong TN, Schulten K. Molecular dynamics simulations suggest that electrostatic funnel directs binding of tamiflu to influenza N1 neuraminidases. PLOS Comput Biol 2010; 6: e1000939.

[86] Mai BK, Li MS. Neuraminidase Inhibitor R-125489 - A Promising Drug for Treating Influenza Virus: Steered Molecular Dynamics Approach. Biochem Biophys Res Commun 2011; 410: 689-691.

[87] Cornell WD, Cieplak P, Bayly CI, *et al.* A 2nd generation force-filed for the simulation of proteins, nucleic-acids, and organic molecules. J Am Chem Soc 1995; 117: 5179-5197.

[88] Masukawa KM, Kollman PA, Kuntz ID. Investigation of neuraminidase-substrate recognition using molecular dynamics and free energy calculations. J Med Chem 2003; 46: 5628-5637.

[89] Rungrotmongkol T, Intharathep P, Malaisree M, *et al.* Susceptibility of antiviral drugs against 2009 influenza A (H1N1) virus. Biochem Biophys Res Comm 2009; 385: 390-394.

[90] Nguyen TT, Mai BK, Li MS. Study of Tamiflu sensitivity to variants of A/H5N1 virus using different force fields. J Chem Info Model 2011; 51: 2266-2276.

[91] Shie JJ, FangJM, Wang SY, *et al.* Synthesis ofTamiflu anditsphosphonate congenerspossessingpotent anti-influenza activity. J Am Chem Soc 2007; 129: 11892.

[92] Udommaneethanakit T, Rungrotmongkol T, Bren U, Frecer V, Stanislav M. Dynamic behavior of avian influenza A virus neuraminidase subtype H5N1in complex with Oseltamivir, Zanamivir, Peramivir, and their phosphonate analogues. J Chem Info Model 2009; 49: 2323-2332.

[93] Du QS, Wang SQ, Chou KC. Analogue inhibitors by modifying oseltamivir based on the crystal neuraminidase structure for treating drug-resistant H5N1 virus. Biochem Biophys Res Commun 2007; 362: 525-531.

[94] Cheng LS, Amaro RE, Xu D, Li WW, Arzberger PW, McCammon JA. Ensemble-based virtual screening reveals potential novel antiviral compounds for avian influenza neuraminidase. J Med Chem 2008; 51: 3878-3894.

[95] Rungrotmongkol T, Frecer V, De-Eknamkul W, Hannongbua S, Miertus S. Design of oseltamivir analogs inhibiting neuraminidase of avian influenza virus H5N1. Antivir Res 2009; 82: 51-58.

[96] Guo XL, Wang JF, Zhu YS, Wei DQ. Recent progress on computer-aided inhibitor design of H5N1 influenza A virus. Curr Comput-Aid Drug 2010; 6: 139-146.

[97] Mitrasinovic PM. Advances in the structure-based design of the influenza A neuraminidase inhibitors. Curr Drug Targets 2010; 11: 315-326.

[98] Wang SQ, Cheng XC, Dong WL, Wang RL, Chou KC. Three new powerful oseltamivir derivatives for inhibiting the neuraminidase of influenza virus. Biochem Biophys Res Commun 2010; 401: 188-191.

[99] Yamashita M, Tomozawa T, Kakuta M, Tokumitsu A, Nasu H, Kubo S. CS-8958, a prodrug of the new neuraminidase inhibitor R-125489, shows long-acting anti-influenza virus activity. Antimicrob Agents Chemother 2009; 53: 186-192.

[100] Kiso M, Kubo S, Ozawa M, *et al.* Efficacy of the new neuraminidase inhibitor CS-8958 against H5N1 influenza viruses. PLoS Pathog 2010; 6: e1000786.

[101] Kiso M, Shinya K, Shimojima M, *et al.* Characterization of oseltamivir-resistant 2009 H1N1 pandemic influenza A viruses. PLoS Pathog 2010; 6: e1001079.

[102] Kubo S, Tomozawa T, Kakuta M, Tokumitsu A, Yamashita M. Laninamivir prodrug CS-8958, a long-acting neuraminidase inhibitor, shows superior anti-influenza virus activity after a single administration. Antimicrob Agents Chemother 2010; 54: 1256-1264.

[103] Sugaya N, Ohashi Y. Long-acting neuraminidase inhibitor laninamivir octanoate (CS-8958) versus oseltamivir as treatment for children with influenza virus infection. Antimicrob Agents Chemother 2010; 54: 2575-2582.

[104] Colizzi F, Perozzo R, Scapozza L, Recanatini M, Cavalli A. Single-molecule pulling simulations can discern active from inactive enzyme inhibitors. J Am Chem Soc 2010; 132: 7361-7371.

[105] Kosztin D, Izrailev S, Schulten K. Unbinding of retinoic acid from its receptor studied by steered molecular dynamics. Biophys J 1999; 76: 188-197.

[106] Isralewitz B, Izrailev S, Schulten K. Binding pathway of retinal to bacterio-opsin: A predict tion by molecular dynamics simulations. Biophys J 1997; 73: 2972-2979.

[107] Wriggers W, Schulten K. Stability and dynamics of G-actin: Back-door water diffusion and behavior of a subdomain 3/4 loop. Biophys J 1997; 73: 624-639.

[108] Wriggers W, Schulten K. Investigating a back door mechanism of actin phosphate release by steered molecular dynamics. Proteins 1997; 35: 262-273.

[109] Niu CY, Xu YC, Xu Y, *et al.* Dynamic mechanism of E2020 binding to acetylcholinesterase: A steered molecular dynamics simulation. J Phys Chem B 2005; 109: 23730-23738.

[110] Shen LL, Shen JH, Luo XM, *et al.* Steered molecular dynamics simulation on the binding of NNRTI to HIV-1 RT. Biophys J 2003; 84: 3547-3563.

[111] ZhangY, Tan HW, Lu YY, Jia ZC, Chen GJ. Ca^{2+} dissociation from the C-terminal EFhandpairin calmodulin: A steered molecular dynamics study. FEBS Lett 2008; 582: 1355-1361.

[112] Yang LJ, Zou J, Xie HZ, Li LL, Wei YQ, Yang SY. Steered molecular dynamics simulations reveal the likelier dissociation pathway of Imatinib from its targeting Kinases c-Kit and Abl. Plos One 2009; 4: e8470.

[113] Sun TG, Li CH, Chen WZ, Wang CX. A novel back-door pathway for glutamine release from GlnBP revealed by steered molecular dynamics simulation. J Mol Struct TheoChem 2009; 905: 51-58.

[114] Snow RW, Guerra CA, Noor AM, Myint HY, Hay SI. The global distribution of clinical episodes of Plasmodium falciparum malaria. Nature 2005; 434: 214-217.

[115] Shen J, Li WH, Liu GX, Tang Y, Jiang HL. Computational Insights into the Mechanism of Ligand Unbinding and Selectivity of Estrogen Receptors. J Phys Chem B 2009; 113: 10436-10444.

[116] Kalikka J, Akola J. Steered molecular dynamics simulations of ligand-receptor interaction in lipocalins. Eur Biophys J Biophy 2011; 40: 181-194.

[117] Weihofen WA, Liu JG, Reutter W, Saenger W, Fan H. Crystal structure of CD26/dipeptidylpeptidase IV in complex with adenosine deaminase reveals a highly amphiphilic interface. J Biol Chem 2004; 279: 43330-43335.

[118] Li C, Shen J, Li WH, Lu CH, Liu GX, Tang Y. Possible ligand release pathway of dipeptidyl peptidase IV investigated by molecular dynamics simulations. Proteins 2011; 79: 1800-1809.

[119] Almlof A, B BO, Aqvist J. Binding affinity prediction with different force fields: Examination of the linear interaction energy method. J Comp Chem 2004; 25: 1242-1254.

[120] Pearlman DA. Evaluating the molecular mechanics poisson-boltzmann surface area free energy method using a congeneric series of ligands to p38 MAP kinase. J Med Chem 2005; 48: 7796-2807.

[121] Steinbrecher T, Case DA, Labahn A. A multistep approach to structure-based drug design: studying ligand binding at the human neutrophil elastase. J Med Chem 2006; 49: 1837-1844.

[122] Zhang D, Gullingsrud J,McCammon JA. Potentials of mean force for acetylcholine unbinding from the alpha7 nicotinic acetylcholine receptor ligand-binding domain. J Am Chem Soc 2006; 128: 3019-3026.

[123] Ytreberg FM. Absolute FKBP binding affnities obtained via nonequilibrium unbinding Simulations. J Chem Phys 209; 130: 164906,.

[124] Hajjar E, Perahia D, Debat H, Nespoulous C, Robert CH. Odorant binding and conformational dynamics in the odorant-binding protein. J Biol Chem 2006; 281: 29929-29937.

[125] Yang K, Liu X, Wang X, Jiang H. A steered molecular dynamics method with adaptive direction adjustments. Biochem Biophys Res Comm 2009; 379: 494-498.

[126] Liu X, Wang X, Jiang H. A steered molecular dynamics method with direction optimization and its applications on ligand molecule dissociation. J Biochem Biophys Methods 2008; 70: 857-864.

[127] Whalen KL, Chang KM, Spies MA. Hybrid steered molecular dynamics-docking: an efficient solution to the problem of ranking inhibitor affinities against a flexible drug target. Mol Inform 2011; 30: 459-471.

[128] Buch I, Giorgino T, Fabritiis GD. Complete reconstruction of an enzyme-inhibitor binding process by molecular dynamics simulations. Proc Natl Acad Sci 2011; 108: 10184-10189.

Received: September 19, 2011 Revised: September 25, 2011 Accepted: September 26, 2011